Synthesis and Cyclic Voltammetric Studies of the Diiron Complexes $ER_2[(\eta^5\text{-}C_5H_4)Fe(L_2)Me]_2$ (E = C, Si, Ge, Sn; R = H, alkyl; L_2 = diphosphine) and $(\eta^5\text{-}C_5H_5)Fe(L_2)ER_2Fc$ (Fc = $(\eta^5\text{-}C_5H_4)Fe(\eta^5\text{-}C_5H_5)$)

Mukesh Kumar,[†] Francisco Cervantes-Lee,[†,‡] Keith H. Pannell,*[,†] and Jianguo Shao[§]

Departments of Chemistry, University of Texas at El Paso, El Paso, Texas 79968-0513, and Midwestern State University, 3410 Taft Boulevard, Wichita Falls, Texas 76308-2099

Received May 5, 2008

Cyclic voltammetric studies on $ER_2[(\eta^5\text{-}C_5H_4)Fe(L_2)Me]_2$ (L_2 = dppe; ER_2 = CH_2 (**1a**), $SiMe_2$ (**2a**), $GeMe_2$ (**3a**), $SnMe_2$ (**4a**)) revealed two well-resolved reversible waves ($^1E_{1/2} = -0.33$ V, $^2E_{1/2} = -0.20$ V (for **1a**); $^1E_{1/2} = -0.35$ V, $^2E_{1/2} = -0.21$ V (for **2a**); $^1E_{1/2} = -0.36$ V, $^2E_{1/2} = -0.23$ V (for **3a**); $^1E_{1/2} = -0.36$ V, $^2E_{1/2} = -0.22$ V (for **4a**)) in CH_2Cl_2, suggesting electronic communication between two iron centers, which is seen for the first time in this family of organometallic complexes. The resolution between two reversible waves increases in the order **1a** < **2a** < **3a** < **4a**; however, coordinating solvents such as pyridine, PhCN, DMSO, and DMF decreased these interactions, attributable to the stabilization of cationic species formed after the first oxidation. UV/vis spectroelectrochemistry of **1a**−**4a** revealed two distinct absorbance patterns for both redox processes and reflected the stepwise oxidation. Homobimetallic complexes containing ferrocenyl groups, $(\eta^5\text{-}C_5H_5)Fe(L_2)ER_2Fc$ (ER_2 = none, L_2 = cis-dppen (**5a**); $ER_2 = SiMe_2$, L_2 = cis-dppen (**6a**), dppm (**6b**); $ER_2 = GeMe_2$, L_2 = cis-dppen (**7a**), dppm (**7b**); $ER_2 = Sn^tBu_2$, L_2 = dmpe (**8a**); Fc = $(\eta^5\text{-}C_5H_4)Fe(\eta^5\text{-}C_5H_5)$), were prepared and studied in terms of electrochemistry. The cyclic voltammogram of **5a** exhibited two well-resolved one-electron reversible waves at $^1E_{1/2} = -0.21$ V and $^2E_{1/2} = 0.58$ V corresponding to oxidation of the Fe(P−P) and Fc iron atoms, respectively. Other complexes in this series (**6a/6b, 7a/7b, 8a**) containing direct Fe−E−Fc (E = Si, Ge, Sn) bridging units were not stable under electrochemical conditions, and rupture of the Fe−E bonds was observed.

Introduction

Organometallic complexes with two or more redox-active transition metals linked by specific bridging spacers are of interest, due to possible electronic communication and mixed-valence behavior.[1] Such materials have potential properties related to semiconductivity, molecular electronics, photo-/electroluminescence, magnetism, and nonlinear optics.[1,2] For example, bis(ferrocenyl) complexes[3−5] bridged by different spacers such as $(SiMe_2)_n$[4] (Figure 1, **C**), $(CH{=}CH)_n$,[5] etc. exhibit electronic interactions depending upon the value of *n*. Similarly, ferrocenylene−silylene polymers, $-[FCSiMe_2]_m-$, have been investigated in detail in terms of electrochemistry,[6] and I_2 doping experiments on thin films of such polymers exhibited mixed-valence character and conducting properties.[6f] Furthermore, Mössbauer spectroscopy of these mixed-valence systems indicated significant thermal transformations from $[FC]^+$ to [FC] due to the presence of the $[I_3]^-$ and $[I_5]^-$ counteranions.[6g]

[†] University of Texas at El Paso.

[‡] Dr. Francisco (Paco) Jose Cervantes-Lee: 11/21/1950−2/15/2007.

[§] Midwestern State University.

(1) (a) *Mixed-Valence Compounds, Theory and Applications in Chemistry, Physics, Geology and Biology*; Brown, D. W., Ed.; Reidel: Boston, MA, 1980. (b) Creutz, C. *Prog. Inorg. Chem.* **1983**, *30*, 1. (c) *Mixed-Valence Compounds*; Brown, D. B., Ed.; Reidel: Boston, MA, 1980. (d) Astruc, D. *Electron-Transfer and Radical Processes in Transition Metal Chemistry*; VCH: New York, 1995; Chapter 1. (e) *Mixed Valency Systems, Applications in Chemistry, Physics and Biology*; Prassides, K., Ed.; Kluwer Academic: Dordecht, The Netherlands, 1991. (f) Demadis, K. D.; Hartshorn, C. M.; Meyer, T. J. *Chem. Rev.* **2001**, *101*, 2655. (g) Kaim, W.; Klein, A.; Glö ckle, M. *Acc. Chem. Res.* **2000**, *33*, 755. (h) Paul, F.; Lapinte, C. *Coord. Chem. Rev.* **1998**, *178−180*, 431. (i) Ziessel, R.; Hissler, M.; El-ghayoury, A.; Harriman, A. *Coord. Chem. Rev.* **1998**, *178−180*, 1251. (j) Astruc, D. *Acc. Chem. Res.* **1997**, *30*, 383.

(2) (a) *Conjugated Polymer Materials: Opportunities in Electronic, Optoelectronic and Molecular Electronics*; Bredas, J. L., Chance, R. R., Eds.; Kluwer: Dordrecht, The Netherlands, 1990; NATO ASI Series, Vol. *182*. (b) Jortner, J.; Ratner, M. A. *Molecular Electronics*; Blackwell Science: Oxford, U.K., 1997. (c) Lehn, J.-M. *Supramolecular Chemistry-Concepts and Perspectives*; VCH: Weinheim, Germany, 1995. (d) Ward, M. D. *Chem. Soc. Rev.* **1995**, *121*. (e) McCleverty, J. A.; Ward, D. *Acc. Chem. Res.* **1998**, *31*, 832. (f) Hoshino, Y.; Higuchi, S.; Fiedler, J.; Su, C.-Y.; Knodler, A.; Schwederski, B.; Sarkar, B.; Hartmann, H.; Kaim, W. *Angew. Chem., Int. Ed.* **2003**, *42*, 674. (g) Patoux, C.; Launay, J.-P.; Beley, M.; Chodorowski-Kimmes, S.; Collin, J.-P.; James, S.; Sauvage, J.-P. *J. Am. Chem. Soc.* **1998**, *120*, 3717. (h) Laye, R. H.; Couchman, S. M.; Ward, M. D. *Inorg. Chem.* **2001**, *40*, 4089. (i) Mosher, P. J.; Yap, G. P. A.; Crutchley, R. J. *Inorg. Chem.* **2001**, *40*, 1189. (j) Cameron, C. C.; Pickup, P. G. *J. Am. Chem. Soc.* **1999**, *121*, 7710. (k) Beck, W.; Niemer, B.; Wieser, M. *Angew. Chem., Int. Ed. Engl.* **1993**, *32*, 923. (l) Hunter, A. D. *Organometallics* **1989**, *8*, 1118. (m) Chukwu, R.; Hunter, A. D.; Santarsiero, B. D. *Organometallics* **1992**, *11*, 589.

(3) (a) Hendrickson, D. N. In *Mixed Valency Systems, Applications in Chemistry, Physics and Biology*; Prassides, K.; Ed.; Kluwer Academic: Dordecht, The Netherlands, 1991; p 67. (b) Barlow, S.; O'Hare, D. *Chem. Rev.* **1997**, *97*, 637. (c) Morrison, W. H., Jr.; Hendrickson, D. N. *Inorg. Chem.* **1975**, *14*, 2331. (d) Moore, M. F.; Wilson, S. R.; Cohn, M. J.; Dong, T.-Y.; Mueller-Westerhoff, U. T.; Hendrickson, D. N. *Inorg. Chem.* **1985**, *24*, 4559. (e) Hendrickson, D. N.; Oh, S. M.; Dong, T.-Y.; Kambara, T.; Cohn, M. J.; Moore, M. F. *Comments Inorg. Chem.* **1985**, *4*, 329. (f) Dong, T.-Y.; Hendrickson, D. N.; Pierpont, C. G.; Moore, M. F. *J. Am. Chem. Soc.* **1986**, *108*, 963. (g) Nakashima, S.; Nishimori, A.; Masuda, Y.; Sano, H.; Sorai, M. *J. Phys. Chem. Solids* **1991**, *52*, 1169. (h) Webb, R. J.; Hagen, P. M.; Wittebort, R. J.; Sorai, M.; Hendrickson, D. N. *Inorg. Chem.* **1992**, *31*, 1791.

10.1021/om8004004 CCC: $40.75
Publication on Web 08/27/2008

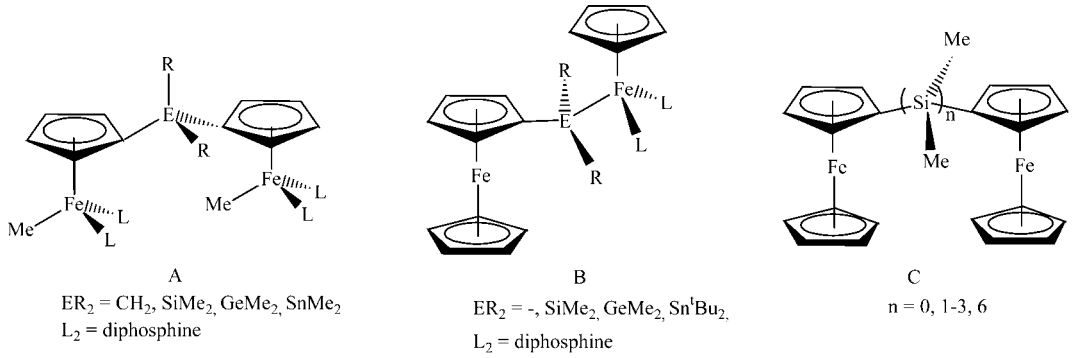

Figure 1. Representation of group 14 element bridged diiron complexes.

Homo and hetero bi-/trimetallic complexes with conjugated and rigid spacers such as −C≡C− and −C≡C−aryl−C≡C− have been utilized with a variety of transition metals and their electrochemical properties in terms of mixed-valence behavior and electron delocalization disclosed.[7] Furthermore, the electrochemical properties of other metal complexes containing redox-active ligands, e.g. tetrathiafulvene,[8] 1,2-dioxalenes,[9] catecholate, semiquinone/quinone[9] and ferrocene-based ligands,[10] have also been evaluated to create an active area of modern organometallic materials chemistry.

Recently we reported the electrochemistry of the monoiron complexes (η^5-C_5H_5)Fe(L_2)ER_3 (L_2 = bis(diphenylphosphino)methane (dppm); $ER_3 = CH_3$, $SiMe_3$, $GeMe_3$, $SnMe_3$)[11] and the 1-sila-3-ferracyclobutanes, [(η^5-C_5H_4)Fe(L_2)CH_2SiMe_2] (L_2 = dppm, dppe, dppp).[12] As part of our continuing interest in such materials, we report the synthesis and electrochemical characteristics of group 14 element bridged bimetallic iron complexes involving the ferrocenyl and cyclopentadienyliron-diphosphine moieties, $ER_2[(\eta^5\text{-}C_5H_4)Fe(L_2)Me]_2$ (E = C, Si, Ge, Sn; R = H, Me; L_2 = diphosphine) and (η^5-C_5H_5)Fe(L_2)ER_2Fc (Fc = (η^5-C_5H_4)Fe(η^5-C_5H_5)) (Figure 1; **A** and **B**).

Results and Discussion

Group A Compounds: $ER_2[(\eta^5\text{-}C_5H_4)Fe(L_2)Me]_2$ (L_2 = dppe; $ER_2 = CH_2$ (1a), $SiMe_2$ (2a), $GeMe_2$ (3a), $SnMe_2$ (4a). Synthesis. The dicarbonyl precursors $ER_2[(\eta^5\text{-}C_5H_4)Fe(CO)_2Me]_2$ ($ER_2 = CH_2$ (**1**), $SiMe_2$ (**2**)) were prepared from the reaction between $ER_2(Fp^-Na^+)_2$ ($Fp = \eta^5$-$C_5H_4Fe(CO)_2$)[13] and iodomethane at low temperature (eq 1). The corresponding complexes $ER_2[(\eta^5\text{-}C_5H_4)Fe(CO)_2Me]_2$ (ER_2 = $GeMe_2$ (**3**), $SnMe_2$ (**4**)) were synthesized by the base-induced double-migration chemistry outlined in eq 2.[14]

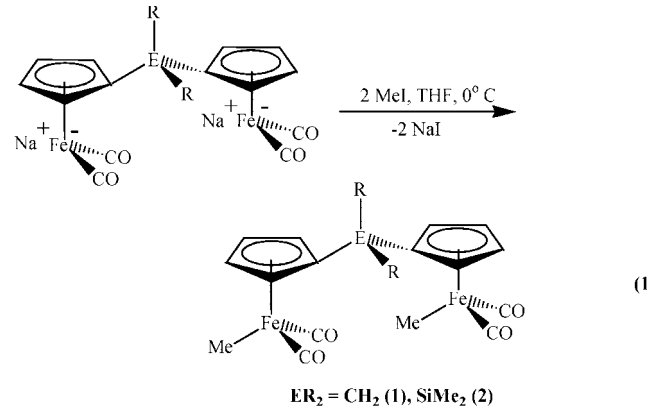

(1)

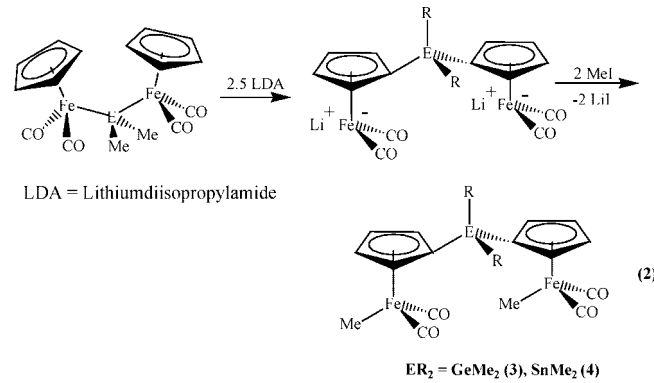

(2)

The initial dicarbonyl complexes, **1–4**, were treated photochemically (2−3 days) with two equivalent of the appropriate

(4) Dement'ev, V. V.; Cervantes-Lee, F.; Parkanyi, L.; Sharma, H.; Pannell, K. H.; Nguyen, M. T.; Diaz, A. *Organometallics* **1993**, *12*, 1983.
(5) Ribou, A.-C.; Launay, J.-P.; Sachtleben, M. L.; Li, H.; Spangler, C. W. *Inorg. Chem.* **1996**, *35*, 3735.
(6) (a) Nguyen, M. T.; Diaz, A. F.; Dementiev, V. V.; Sharma, H. K.; Pannell, K. H. *SPIE Proc.* **1993**, *1910*, 230. (b) Nguyen, M. T.; Diaz, A. F.; Dementiev, V. V.; Pannell, K. H. *Chem. Mater.* **1993**, *5*, 1389. (c) Nguyen, M. T.; Diaz, A. F.; Dementiev, V. V.; Pannell, K. H. *Chem. Mater.* **1994**, *6*, 952. (d) Foucher, D. A.; Tang, B.-Z.; Manners, I. J. *J. Am. Chem. Soc.* **1992**, *114*, 6246. (e) Rulkens, R.; Lough, A. J.; Manners, I.; Lovelace, S. R.; Grant, C.; Geiger, W. E. *J. Am. Chem. Soc.* **1996**, *118*, 12683. (f) Espada, L.; Pannell, K. H.; Papkov, V.; Leites, L.; Bukalov, S.; Suzdalev, I.; Tanaka, M.; Hayashi, T. *Organometallics* **2002**, *21*, 3758. (g) Pannell, K. H.; Imshennik, V. I.; Maksimov, Yu. V.; Il'ina, M. N.; Sharma, H. K.; Papkov, V. S.; Suzdalev, I. P. *Chem. Mater.* **2005**, *17*, 1844.
(7) (a) Akita, M.; Tanaka, Y.; Naitoh, C.; Ozawa, T.; Hayashi, N.; Takeshita, M.; Inagaki, A.; Chung, M. *Organometallics* **2006**, *25*, 5261. (b) De Montigny, F.; Argouarch, G.; Costuas, K.; Halet, J.; Roisnel, T.; Toupet, L.; Lapinte, C. *Organometallics* **2005**, *24*, 4558. (c) Chen, J.-L.; Zhang, L.-Y.; Chen, Z.-N.; Gao, L.-B.; Abe, M.; Sasaki, Y. *Inorg. Chem.* **2004**, *43*, 1481. (d) Sato, M.; Hayashi, Y.; Kumakura, S.; Shimizu, N.; Katada, M.; Kawata, S. *Organometallics* **1996**, *15*, 721. (e) Weyland, T.; Lapinte, C.; Frapper, G.; Calhorda, M. J.; Halet, J.-F.; Toupet, L. *Organometallics* **1997**, *16*, 2024. (f) Weyland, T.; Costuas, K.; Toupet, L.; Halet, J.-F.; Lapinte, C. *Organometallics* **2000**, *19*, 4228. (g) Bruce, M. I.; De Montigny, F.; Jevric, M.; Lapinte, C.; Skelton, B. W.; Smith, M. E.; White, A. H. *J. Organomet. Chem.* **2004**, *689*, 2860. (h) Coat, F.; Guillemot, M.; Paul, F.; Lapinte, C. *J. Organomet. Chem.* **1999**, *578*, 76. (i) Alberto, C.; Saverio, S.; Laura, O.; Annalisa, B. *Coord. Chem. Rev.* **2004**, *248*, 683. (j) Wong, C.-Y.; Che, C.-M.; Chan, M. C. W.; Leung, K.-H.; Phillips, D. L.; Zhu, N. *J. Am. Chem. Soc.* **2004**, *126*, 2501.
(8) Gouverd, C.; Biaso, F.; Cataldo, L.; Berclaz, T.; Geoffroy, M.; Levillain, E.; Avarvari, N.; Fourmigue, M.; Sauvage, F. X.; Wartelle, C. *Phys. Chem. Chem. Phys.* **2005**, *7*, 85.
(9) (a) Meacham, A. P.; Druce, K. L.; Bell, Z. R.; Ward, M. D.; Keister, J. B.; Lever, A. B. P. *Inorg. Chem.* **2003**, *42*, 7887. (b) Pierpont, C. G.; Lange, C. W. *Prog. Inorg. Chem.* **1994**, *41*, 331. (c) Ward, M. D.; McCleverty, J. A. *Dalton Trans.* **2002**, 275.
(10) Ohs, A. C.; Rheingold, A. L.; Shaw, M. J.; Nataro, C. *Organometallics* **2004**, *23*, 4655.
(11) Kumar, M.; Reyes, E. A.; Pannell, K. H. *Inorg. Chim. Acta* **2008**, *361*, 1793.

diphosphine to form the redox-active complexes, **1a**−**4a**, in 60−70% yield, eq 3.

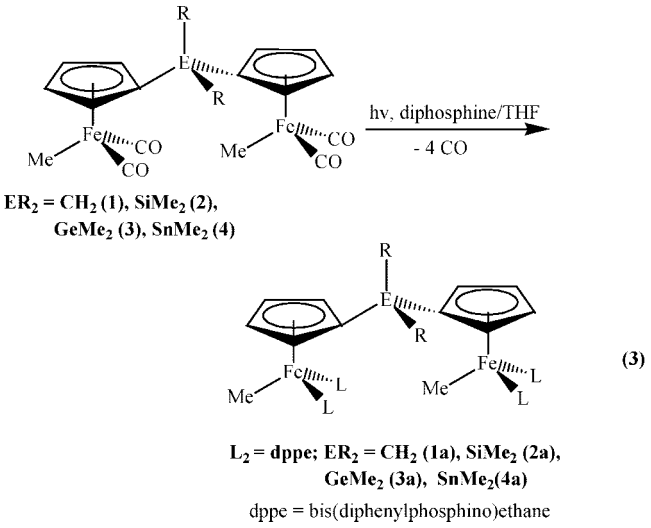

(3)

The photochemical reactions were monitored by ^{31}P NMR and IR spectroscopy and the stepwise CO substitutions could be observed; however, we made no attempt to isolate the intermediate complexes formed during this process. The desired compounds were isolated as red-orange solid materials soluble in common organic solvents and were characterized by NMR and elemental analysis.

Spectroscopic Characterization. NMR spectroscopic analyses of **1**−**4** and **1a**−**4a** are in total accord with their proposed structures and are presented in the Experimental Section. Thus, as expected, ^{13}C NMR spectra of **1a**−**4a** exhibited triplets for the Fe−Me carbon due to heteronuclear coupling with two equivalent P atoms and appeared in the range of −17.0 to −21.0 ppm. Decoupled ^{31}P NMR spectra exhibited a single resonance for each compound in the range of 109.0−113 ppm, which is ∼130 ppm downfield as compared to resonances for the uncoordinated diphosphine and are comparable to that observed for $[(\eta^5\text{-}C_5H_4)Fe(dppe)CH_2SiMe_2]$[12] and other diphosphine derivatives of iron.[7b,e,15] ^{29}Si and ^{119}Sn NMR resonances for **2a** and **4a** appeared at δ −5.9 and −27.5 ppm, respectively, exhibiting the expected chemical shift differences as compared to resonances for **2** and **4**.[11]

Cyclic Voltammetry. The cyclic voltammograms of the dicarbonyl derivatives **1**−**4** showed only one irreversible oxidation in the range of 1.2−1.4 V (TBAP/dichloromethane, GCE), typical of the Fp [Fp = $(\eta^5\text{-}C_5H_5)Fe(CO)_2$] derivatives.[11,16] No apparent intramolecular communication between the two Fe atoms is observed prior to decomposition; however, the oxidation wave is quite broad compared to those of related reversible systems and probably contains several distinct processes. On the other hand, compounds **1a**−**4a** exhibited two reversible waves (Figure 2). The CH_2-bridged complex **1a** showed a weakly resolved pair of reversible waves, and they

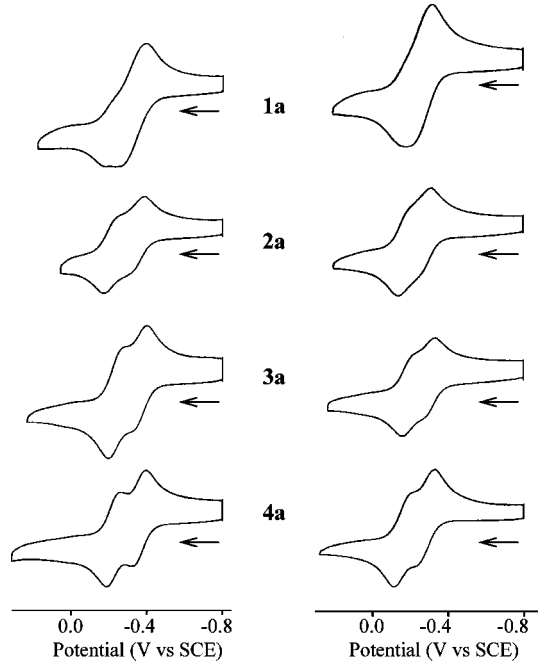

Figure 2. Cyclic voltammograms for **1a**−**4a** in CH_2Cl_2 (left) and pyridine (right).

were identified at $^1E_{p,a} = -0.26$ V and $^2E_{p,a} = -0.17$ V in dichloromethane (Table 1). Surprisingly, the difference between the two oxidation values $^1E_{p,a}$ and $^2E_{p,a}$ ($\Delta E_{p,a}$) changes relatively little as a consequence of changing the nature of the group 14 bridge, although the resolution between the two increases in the order C < Si < Ge < Sn. The same is true for the half-wave potential values ($E_{1/2}$).

The difference between the two redox processes can be expressed as $\Delta E_{1/2}$ (V) = $^2E_{1/2} - {}^1E_{1/2}$, where $E_{1/2} = (E_{p,a} + E_{p,c})/2$, and in general this value is similar to the simpler ΔE_{pa} ($^2E_{p,a} - {}^1E_{p,a}$). For complexes **1a**−**4a** such values are in the range 0.09−0.14 V with the single-atom bridges. In comparison, the series of bis(ferrocenyl)polyenes $Fc(CH{=}CH)_nFc$ exhibited $\Delta E_{1/2} = 0.17$ V ($n = 1$), 0.12 V ($n = 2$),[5] whereas the class **C** compounds $Fc(SiMe_2)_nFc$[4] had values of $\Delta E_{p,a} = 0.34$ V ($n = 0$), 0.15 V ($n = 1$), 0.11 ($n = 2$), 0.08 V ($n = 3$). These data reveal that the extent of electronic communication between two iron atoms is much higher when $n = 0$ and quickly decreases as n increases. Thus, the present complexes compare reasonably with those noted above. However, in comparison, the 1,1-ferrocenophanes $[(\eta^5\text{-}C_5H_4)Fe(\eta^5\text{-}C_5H_4ER_2)]_2$ were reported to have larger $\Delta E_{1/2}$ (V) values as compared to those of **1a**−**4a**: $ER_2 = CH_2$, 0.20;[17] Sn^nBu_2, 0.20;[18] $SiMe_2$, 0.25;[19] Sn^tBu_2, 0.27;[20] $SnMes_2$, 0.28;[20] $PbPh_2$, 0.2.[21]

The use of the more coordinating solvent pyridine resulted in both a decrease in the resolution of the waves and a reduction in the oxidation potentials for the various processes. To determine the solvent effect on the difference between the two oxidation potentials, cyclic voltammograms for compound **4a**

(12) Kumar, M.; Cervantes-Lee, F.; Sharma, H. K.; Pannell, K. H. *Organometallics* **2007**, *26*, 3005.
(13) (a) Zhang, Y.; Cervantes-Lee, F.; Pannell, K. H. *J. Organomet. Chem.* **2001**, *634*, 102. (b) Bitterwolf, T. E. *J. Organomet. Chem.* **1996**, *312*, 197.
(14) Sharma, S.; Cervantes, J.; Mata-Mata, J. L.; Brun, M.-C.; Cervantes-Lee, F.; Pannell, K. H. *Organometallics* **1995**, *14*, 4269.
(15) Scott, F.; Kruger, G. J.; Cronje, S.; Lombard, A.; Raubenheimer, H. G. *Organometallics* **1990**, *9*, 1071.
(16) Geiger, W. E. Organometallic Electrochemistry: Origins, Development, and Future. *Organometallics* **2007**, *26*, 5738.
(17) Diaz, A. F.; Müller-Westerhoff, U. T.; Nazzal, A.; Tanner, M. *J. Organomet. Chem.* **1982**, *236*, C45.
(18) Dong, T.-Y.; Hwang, M.-Y.; Wen, Y.-S.; Hwang, W.-S. *J. Organomet. Chem.* **1990**, *391*, 377.
(19) Zechel, D. L.; Foucher, D. A.; Pudelski, J. K.; Yap, G. P. A.; Rheingold, A. L.; Manners, I. *J. Chem. Soc., Dalton Trans.* **1995**, *1893*.
(20) Jäkle, F.; Rulkens, R.; Zech, G.; Foucher, D. A.; Lough, A. J.; Manners, I. *Chem. Eur. J.* **1998**, *4*, 2117.
(21) Utri, G.; Schwarzhans, K.-E.; Allmaier, G. M. *Z. Naturforsch., B* **1990**, *45*, 755.

Table 1. Electrochemical Data of 1a−4a in CH_2Cl_2 and Pyridine Containing 0.1 M TBAP

compd	solvent	$^1E_{p,a}$	$^1E_{p,c}$	$^1E_{1/2}$	$^2E_{p,a}$	$^2E_{p,c}$	$^2E_{1/2}$	$\Delta E_{1/2}{}^a$	$\Delta E_{p,a}{}^b$	K_c
1a	CH_2Cl_2	−0.26	−0.39	−0.33	−0.17	−0.23	−0.20	0.13	0.09	172
2a		−0.30	−0.40	−0.35	−0.17	−0.25	−0.21	0.14	0.13	256
3a		−0.32	−0.39	−0.36	−0.19	−0.27	−0.23	0.13	0.13	172
4a		−0.32	−0.40	−0.36	−0.18	−0.26	−0.22	0.14	0.14	256
1a	pyridine	−0.20	−0.32	−0.26	−0.14	−0.20	−0.17	0.09	0.06	4
2a		−0.26	−0.32	−0.29	−0.14	−0.20	−0.17	0.12	0.12	116
3a		−0.27	−0.33	−0.30	−0.15	−0.23	−0.19	0.11	0.12	78
4a		−0.25	−0.33	−0.29	−0.13	−0.21	−0.17	0.12	0.12	116

^{a} $\Delta E_{1/2}$ (V) $= {}^2E_{1/2} - {}^1E_{1/2}$. ^{b} $\Delta E_{p,a}$ (V) $= {}^2E_{p,a} - {}^1E_{p,a}$.

were recorded using the polar solvents PhCN, DMF, and DMSO. A significant correlation exists between the solvent dielectric constant and $\Delta E_{1/2}$: the more polar the solvent, the smaller the separation, e.g. variations from 90 mV in DMF to 140 mV in CH_2Cl_2 (see the figure in the Supporting Information). The better the stabilization of the initially formed charge by the solvent, the lesser the impact of that charge upon the neighboring metal center oxidation process.[22]

The comproportionation associated with the reaction for a class II system is shown in eq 4.

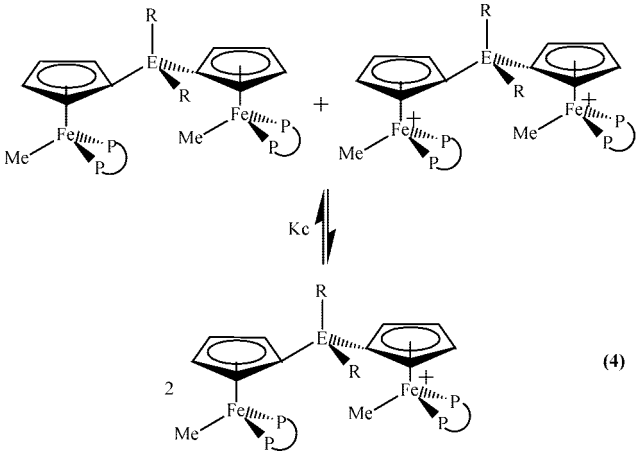

(4)

The K_c values were calculated by using the $e[({}^2E_{1/2} - {}^1E_{1/2})n_1n_2F]/RT$ relationship ($n_1 = n_2 = 1$; F = Faraday constant, R = gas constant, $T = 293$ K).[23] As shown in Table 1, the values for K_c (CH_2Cl_2), in the range 170−260, are greater than those for [{Cp*(dppe)Fe(−C≡C−)}$_2$(1,3-C_6H_4)] (K_c = 130) and [{Cp*(dppe)Fe(−C≡C−)}$_3$(1,3,5-C_6H_3)] (K_c = 130).[7f] These data suggest that for complexes **1a**−**4a** the equilibrium favors mixed-valence species.

UV/Vis Spectroelectrochemistry of 1a−4a. A UV/vis spectroelectrochemical study of **1a**−**4a** was performed in the region 300−1100 nm. The spectral changes of both **1a** and **4a** upon oxidation are available in the Supporting Information. Compound **1a** showed four isosbestic points at 324, 430, 508, and 578 nm for the first oxidation at −0.20 V, while for the second oxidation process at 0.0 V three isosbestic points at 326, 426, and 497 nm are observed. Similar behavior was noted for **2a**−**4a**. All spectral variations are reversible, as are the electrochemical processes. However, due to the small changes in molar absorptivity of these compounds, no significant conclusions about the electronic transitions could be made at this time (see the figure in the Supporting Information). We observed no well-defined near-IR bands in the region 800−1100 nm but the region 1100−2500 nm was not examined.

Group B compounds: (η^5-C_5H_5)Fe(L$_2$)ER$_2$Fc (ER$_2$ = none, L$_2$ = cis-dppen (5a); ER$_2$ = SiMe$_2$, L$_2$ = cis-dppen (6a), dppm (6b); ER$_2$ = GeMe$_2$, L$_2$ = cis-dppen (7a), dppm (7b); ER$_2$ = Sn^{t}Bu$_2$, L$_2$ = dmpe (8a); Fc = (η^5-C_5H_4)Fe(η^5-C_5H_5)). Synthesis and Characterization. Compound **5**, containing a direct ferrocenyl−iron bond, was prepared by the salt-elimination reaction between FcLi and FpI (Fc = η^5-$C_5H_4FeC_5H_5$, Fp = (η^5-C_5H_5)Fe(CO)$_2$)[24] (eq 5). Synthesis of **6**−**8** involved quenching Fp^-Na^+ with FcECl (E = $SiMe_2$, $GeMe_2$, Sn(^{t}Bu)$_2$)[25] (eq 6). The synthesis of FcECl was achieved in good yield using the procedure reported in the literature involving the reaction of corresponding 1-ferrocenophane with HCl.[26] Infrared, ^{1}H, ^{13}C, ^{29}Si, and ^{119}Sn NMR spectroscopic analysis were in accord with their structural formulation, and the data are presented in the Experimental Section.

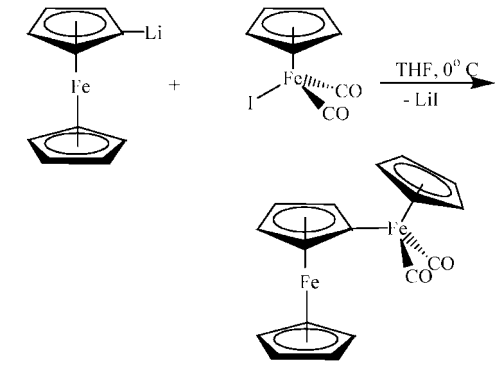

(5)

5

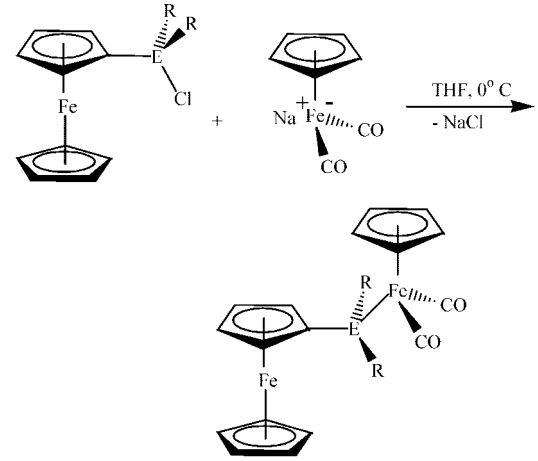

(6)

ER$_2$ = SiMe$_2$ (6) , GeMe$_2$ (7), Sn(^{t}Bu)$_2$ (8)

Ultraviolet irradiation of **5**−**8** in the presence of a diphosphine (24−36 h) resulted in the formation of the expected CO-substituted products (eq 7). These reactions were monitored by

(22) (a) Chen, P.; Meyer, T. J. *Chem. Rev.* **1998**, *98*, 1439. (b) Barriere, F.; Geiger, W. E. *J. Am. Chem. Soc.* **2006**, *128*, 3980.

(23) (a) Sutton, J. E.; Taube, H. *Inorg. Chem.* **1981**, *20*, 3125. (b) Sutton, J. E.; Sutton, P. M.; Taube, H. *Inorg. Chem.* **1979**, *18*, 1017. (c) Creutz, C. *Prog. Inorg. Chem.* **1983**, *30*, 1.

IR and ^{31}P NMR spectroscopy and showed the stepwise replacement of the CO groups; however, we made no attempt to isolate the monosubstituted materials. The diphosphine derivatives **5a**, **6a/6b**, **7a/7b**, and **8a** were isolated as orange-red solid materials and purified by recrystallization from toluene/hexane mixtures.

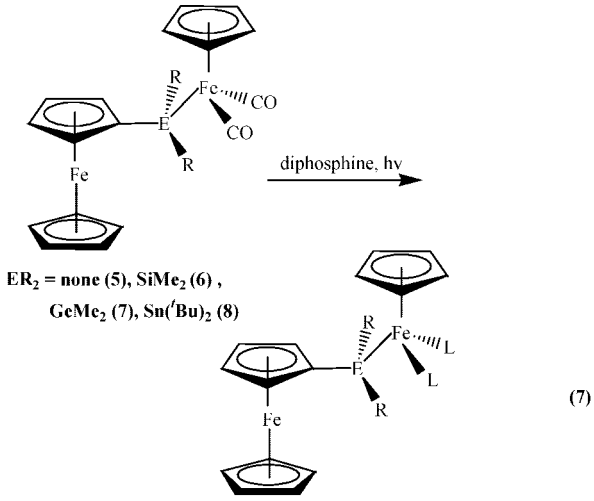

(7)

ER_2= none, L_2 = cis-dppen (5a)

ER_2 = $SiMe_2$, L_2 = cis-dppen (6a), dppm (6b)

ER_2 = $GeMe_2$, L_2 = cis-dppen (7a), dppm (7b)

ER_2 = $Sn(^tBu)_2$,L_2 = dmpe (8a)

cis-dppen = Bis(diphenylphosphino)ethylene
dppm = Bis((diphenylphosphino)methane
dmpe= Bis((dimethylphosphino)ethane

The ^1H and ^{13}C NMR spectral properties of the new complexes are in accord with their proposed structures. The ^{29}Si NMR spectra of both **6a** and **6b** showed a triplet due to two-bond heteronuclear coupling for the *Si*FeP_2 moiety (26.0 ppm, $^2J_{Si-P}$ = 45.7 Hz (**6a**); 26.7 ppm, $^2J_{Si-P}$ = 44.5 Hz (**6b**)), reflecting the expected moderate upfield shift when compared to **6** (36.2 ppm).[25] Similarly, a triplet ($^2J_{Sn-P}$ = 409 Hz) in the ^{119}Sn NMR spectrum of **8a** was observed at 105.2 ppm. ^{31}P NMR spectra of all these compounds showed a downfield shift as compared to free phosphine ligands.

Crystal Structure of 6b. There is apparently only a single literature report concerning the structures of $Fp(L_2)R$ complexes, that of Fp(dppm)Ph.[27] The structural data reveal a piano-stool arrangement at the Fe atom with Fe−P1 and Fe−P2 bond distances of 2.199(1) and 2.174(1) Å, respectively, with a P1−Fe−P2 bite angle of 73.8(0)°.

The molecular structure of **6b**, as determined by single-crystal X-ray analysis of a crystal formed from a benzene/hexane solvent mixture, also exhibits a piano-stool arrangement at Fe, as shown in Figure 3. The crystallographic data and selected bond lengths and angles are summarized in Tables 2 and 3, respectively. Compound **6b** crystallizes in a monoclinic crystal system with the *C*2/*c* space group, and each molecule in the unit cell crystallizes with 1.5 molecules of C_6H_6; however, the benzene molecule has no apparent interactions with the iron complex.

The Fe2−Si distance of 2.3786(8) Å is reminiscent of distances in the related dicarbonyl complexes [(η^5-C_5H_5)-$Fe(CO)_2]_2Si_2Me_4$ (Fe−Si = 2.375(2) Å),[28] (η^5-C_5H_5)$Fe(CO)_2$-$SiMe_2SiPh_3$ (Fe−Si = 2.346(1) Å),[29] and (η^5-C_5H_5)Fe-$(CO)_2SiMe_2GePh_3$ (Fe−Si = 2.328(1) Å).[30] The geometry around the Si atom is that of a slightly distorted tetrahedron (C41−Si−C42 = 103.22(12), C42−Si−C2 = 100.66(12), C41−Si−C2 = 103.75(12)°). The Fe−P bond distances are 2.1921(7) and 2.1872(7) Å, and the P2−Fe2−P1 bite angle is found to be 74.44(3)°. Such values are almost identical with those noted above for Fp(dppm)Ph[27] and also those observed

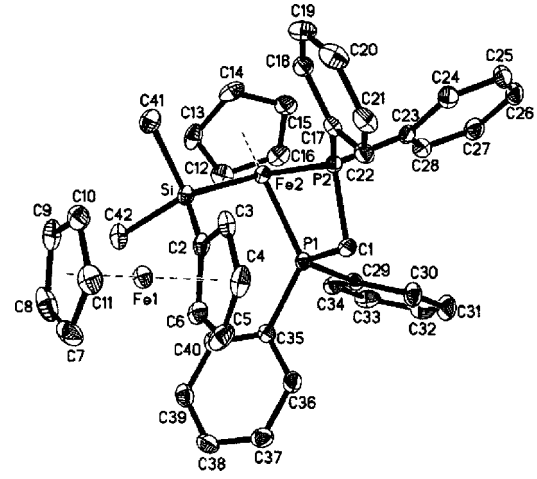

Figure 3. ORTEP diagram of [(η^5-C_5H_5)$Fe(Ph_2PCH_2Ph_2P)SiMe_2Fc$] (**6b**). Thermal ellipsoids are drawn at the 50% probability level, and hydrogen atoms are deleted for clarity.

Table 2. Summary of Crystallographic Data of 6b and 9

	6b	**9**
source	synthesis	synthesis
cryst color	red	red
cryst habit	red chunk	red chunk
cryst size/mm^3	0.20 × 0.16 × 0.16	0.40 × 0.40 × 0.34
a/Å	10.1001(7)	12.3242(12)
b/Å	14.4739(9)	12.3981(12)
c/Å	15.7609(11)	19.5110(19)
α/deg	77.5740(10)	90
β/deg	80.2480(10)	98.403(2)
γ/deg	76.3780(10)	90
volume/Å^3	2169.6(3)	2949.2(5)
cryst syst	monoclinic	monoclinic
space group	*C*2/*c*	$P2_1/c$
Z	2	4
D_c/g cm^{-3}	1.325	1.303
μ/mm^{-1}	0.805	0.681
abs cor	Bruker SADABS V2.05	
temp/K	296(2)	
wavelength (Å)	0.710 73	
monochromator	graphite	
diffractometer	Bruker APEX CCD area detector	
no. of rflns collected	13 475	33 312
no. of indep rflns	9341 (R(int) = 0.0206)	7029 (R(int) = 0.0353)
structure solun technique	direct methods	
structure solution program	SHELXS-97 (Sheldrick, 1990)	
refinement technique	full-matrix least squares on F^2	
refinement program	SHELXL-97 (Sheldrick, 1997)	
function minimized	$\sum w(F_o^2 - F_c^2)^2$	
goodness of fit on F^2	1.047	1.155
R1, wR2 ($I > 2\sigma(I)$)	R1 = 0.0486, wR2 = 0.1068	R1 = 0.0682, wR2 = 0.1586
R1, wR2 (all data)	R1 = 0.0557, wR2 = 0.1112	R1 = 0.0769, wR2 = 0.1643

(24) Pannell, K. H.; Cassias, J. B.; Crawford, G. M.; Flores, A. *Inorg. Chem.* **1976**, *15*, 2671.
(25) Pannell, K. H.; Sharma, H. *Organometallics* **1991**, *10*, 954.
(26) MacLachlan, M. J.; Ginzburg, M.; Zheng, J.; Knoll, O.; Lough, A. J.; Manners, I. *New J. Chem.* **1998**, *22*, 1409.
(27) Scott, F.; Kruger, G. J.; Cronje, S.; Lombard, A.; Raubenheimer, H. G. *Organometallics* **1990**, *9*, 1071.
(28) Pannell, K. H.; Cervantes, J.; Parkanyi, L.; Cervantes-Lee, F. *Organometallics* **1990**, *9*, 859.

Table 3. Selected Bond Lengths (Å) and Angles (deg) of (η^5-C_5H_5)Fe(dppm)$SiMe_2$Fc (6b) and (η^5-C_5H_5)Fe(dppm)$SiMe_3$ (9)

Bond Lengths (Å)

Compound **6b**

Fe2−Si	2.3786(8)	Fe2−P1	2.1921(7)	Fe2−P2	2.1872 (7)
Si−C2	1.924(3)	Si−C41	1.920 (3)	Si−C42	1.921(3)
Fe2−C12	2.114 (3)	Fe2−C13	2.102 (3)	Fe2−C14	2.126 (3)
Fe2−C15	2.128(3)	Fe2−C16	2.128 (3)		

Compound **9**

Fe−Si	2.4756(10)	Fe−P1	2.2789(9)	Fe−P2	2.0878(9)
Si−C31	1.952(4)	Si−C32	1.812(4)	Si−C33	1.929(4)
Fe−C1	1.987(4)	Fe−C2	2.263(3)	Fe−C3	2.126(3)
Fe−C4	2.038(3)	Fe−C5	1.837(3)		

Bond Angles (deg)

Compound **6b**

P2−Fe2−P1	74.44(3)	P1−Fe2−Si	93.76(3)
P2−Fe2−Si	94.06(3)	C41−Si−C2	103.75(12)
C42−Si−C2	100.66(12)	C41−Si−C42	103.22(12)

Compound **9**

P2−Fe−P1	67.35(3)	P1−Fe−Si	100.18(3)
P2−Fe−Si	105.30(3)	C32−Si−C33	110.0(2)
C32−Si−C31	99.0(2)	C33−Si−C31	90.1(2)
C32−Si−Fe	112.11(15)	C33−Si−Fe	116.74(15)
C31−Si−Fe	125.97(13)	P1−C6−P2	85.27(13)

in $Fe(CO)_3$dppm[31] (P1−Fe−P2 = 73.5(1)°; Fe−P1 = 2.209(4) Å, Fe−P2 = 2.225(3) Å). Related bidentate phosphine complexes with larger chelate rings do, as expected, have much larger bite angles: e.g., Cp*(dppe)Fe−C≡C−9,10-ant−C≡C−FeCp*(dppe)[7b] (85.42(5)°), [Cp*Fe(dppe)]$_3$(C≡C)$_3$(μ-1,3,5-C_6H_3)[7e] (84.7(1), 83.7(4), 85.7(1)°), and Fc−C≡C−CpFe(dppe)[7d] (86.7(2)°) (ant = anthracene, dppe = bis(diphenylphosphino)ethane).

The X-ray structure determination of the monoiron analogue (η^5-C_5H_5)Fe(dppm)$SiMe_3$ (**9**) (see ref 11 for the synthesis of **9**) was also performed in order to compare the variations in structural pattern of Fe−Si/Fe−P bond distances and P−Fe−P bite angles (Figure 4, Tables 2 and 3). The differences between the structures of **6b** and **9** are associated with the Fe−Si/Fe−P bond distances and P−Fe−P bite angles. The Fe−Si bond distance observed for **9** (Fe−Si = 2.4756(10) Å) is significantly longer than other reported Fe−Si bond lengths and obviously that found in **6b**, 2.3786(8) Å. Similarly, the two Fe−P bond distances Fe−P1 = 2.2789(9) Å and Fe−P2 = 2.0878(9) Å exhibit a distinct variation from those in **6b** and Fp(dppm)Ph[27] and exhibit a greater Fe−P bond distance difference. It may also be noted that the P1−Fe−P2 bite angle in this complex is sharply reduced to 67.35(3)°. The replacement of one methyl by a ferrocenyl on the trimethylsilyl group gives rise to a large variation in the crystal structure parameters. The extra crowding around the Fe atom of the Fp group results in shorter Fe−Si bond length, an increased bite angle, and a general increase in asymmetry at the Fe center, as noted by two differing Fe−P bond distances.

Cyclic Voltammetry and UV/Vis Spectroelectrochemistry of (η^5-C_5H_5)Fe(cis-dppen)Fc (5a). The cyclic voltammogram of (η^5-C_5H_5)Fe(cis-dppen)Fc (**5a**) in dichloromethane containing 0.1 M TBAP from −0.5 to 1.0 V (vs SCE) revealed two well-separated one-electron reversible redox processes at $E_{1/2}$ = −0.21 and 0.58 V with an $i_{p,a}/i_{p,c}$ current ratio of 1.0. These processes were assigned to the iron centers in the Fp and Fc moieties, respectively (Figure 5). The first oxidation of the Fp moiety makes the ferrocenyl group more difficult to oxidize, as found by comparison with the oxidation potential of the pure ferrocene, 0.54 V (vs SCE). This can be accounted for by either a weak communication between the two metal centers or an electronic effect of the Fp substituent on the Fc center.

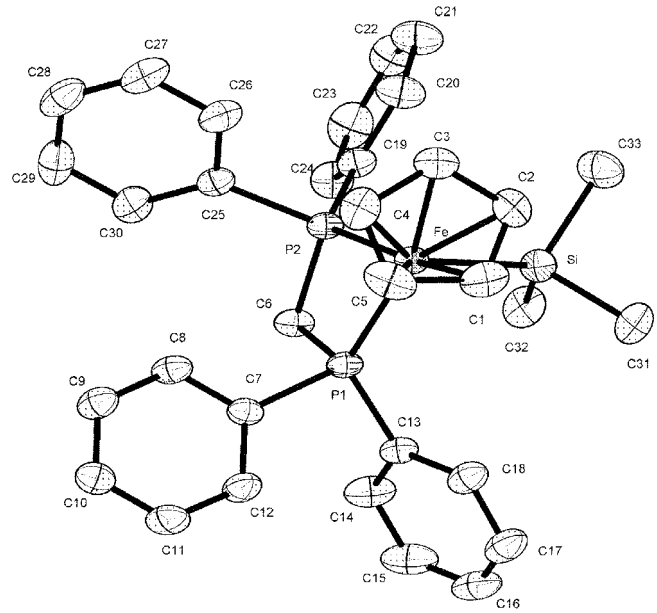

Figure 4. ORTEP diagram of [(η^5-C_5H_5)Fe($Ph_2PCH_2Ph_2P$)$SiMe_3$] (**9**). Thermal ellipsoids are drawn at the 50% probability level, and hydrogen atoms are deleted for clarity.

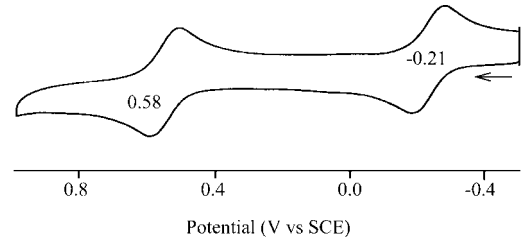

Figure 5. Cyclic voltammogram of (η^5-C_5H_5)Fe(cis-dppen)Fc (**5a**) in CH_2Cl_2 containing 0.1 M TBAP.

Complex **5a** exhibited a clean UV/vis spectroelectrochemistry, as illustrated in Figure 6. The first oxidation at 0.20 V revealed two isosbestic points at 314 and 402 nm. A broad and intense band is formed between 402 and 700 nm. The magnitude of the absorbance associated with the low-energy band in the spectra is strongly suggestive of a charge transfer between the Fc and Fp(P−P) groups that occurs after the first oxidation of the Fp(P−P) moiety. These low-energy bands may be best described as LMCT bands.[7b] The second oxidation at 0.80 V (Figure 6b) also exhibited two isosbestic points at 480 and 750 nm; however, the spectral pattern is different from that expected for a simple Fc/Fc^+ transformation. Interestingly, after the second oxidation, there is a significant reduction in the absorbance in the region of the CT bands.

Cyclic Voltammetry of 6a/6b, 7a/7b, and 8a. Cyclic voltammograms of compounds **6a** and **6b**, containing a dimethylsilyl bridging group between the Fp(P−P) and Fc moieties, were obtained in dichloromethane/TBAP solution. The results for **6a** are illustrated in Figure 7 and reveal three oxidations, and that of **6b** is similar (Table 4). A first reversible oxidation at ∼0.0 V is reminiscent of those noted above for

(29) Parkanyi, L.; Pannell, K. H.; Hernandez, C. *J. Organomet. Chem.* **1983**, *252*, 127.
(30) Parkanyi, L.; Hernandez, C.; Pannell, K. H. *J. Organomet. Chem.* **1986**, *301*, 145.
(31) Cotton, F. A.; Hardcastle, K. I.; Rusholme, G. A. *J. Coord. Chem.* **1973**, *2*, 217.

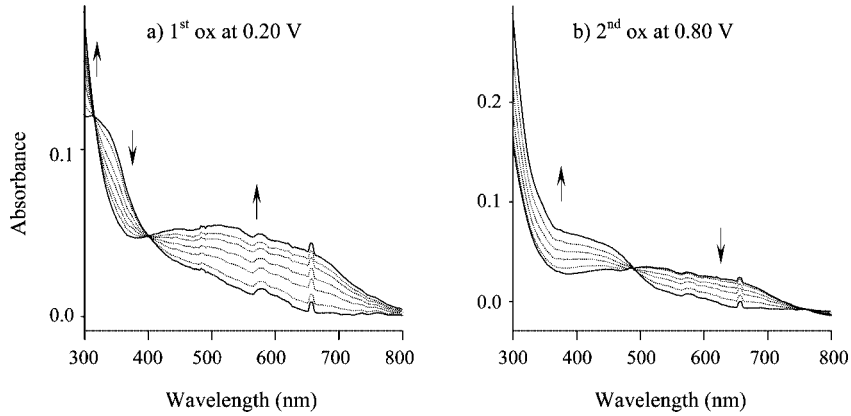

Figure 6. UV/vis spectral changes for (η^5-C_5H_5)Fe(cis-dppen)Fc (**5a**) upon the first (a) and the second (b) oxidations in CH_2Cl_2 containing 0.2 M TBAP.

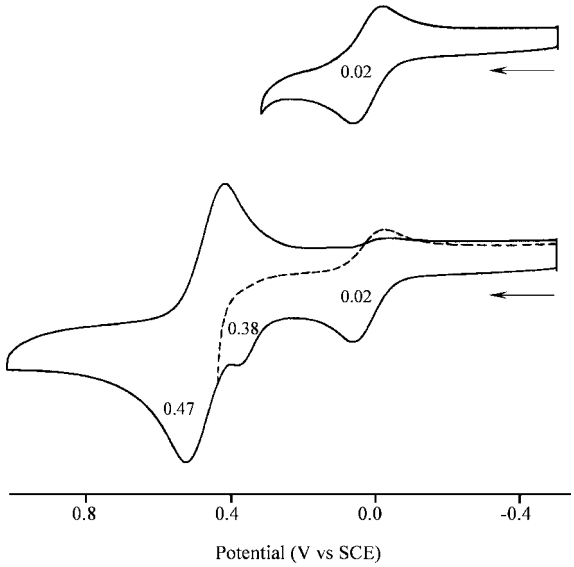

Figure 7. Cyclic voltammograms of (η^5-C_5H_5)Fe(cis-dppen)-$SiMe_2$Fc (**6a**) in CH_2Cl_2 containing 0.1 M TBAP.

the Fp(P−P) part of the molecule, and the third reversible oxidation in the region of ∼0.5 V is typical of those associated with a ferrocenyl group. However, the system is neither simple nor clean. Recycling the electrochemistry process illustrates that the initial Fp(P−P) reversible oxidation disappears. After the initial oxidation of the Fp(P−P) group, there appears to be a cleavage of the Fe−Si bond in these complexes under these conditions. The chemical decomposition is slow compared to the electrochemical reversibility, but continued spectral observation of the initially formed oxidation product illustrates the slow decomposition.

Related cyclic voltammetric studies on the germyl-bridged bimetallic complexes **7a/7b** showed four oxidations (TBAP, GCE, PtE), the first three of which resemble those observed for **6a** and **6b.** The reason for the appearance of a fourth oxidation is unclear and further illustrates the facile cleavage and decomposition of Fe−metalloid bonds, as observed for the silyl complexes discussed above. The organotin analogue **8a** revealed two irreversible redox in the Fp(P−P) region and one reversible wave observed in the Fc region, all of which are of uncertain provenance but seem to indicate a lesser stability of the particular Fe−Sn bond upon oxidation.

The spectroelectrochemical UV/vis data associated with the above processes confirm the above analysis. The spectral changes observed with the first redox processes for **6a/6b** and **7a/7b** at ∼0.0.V are essentially identical, and a representative spectroelectrogram of **6b** is shown in Figure 8a. Maintaining the oxidation potential in the experiment at 0.25 V, i.e. well below the potential where the subsequent oxidations become significant, results in a well-defined reversible optical change (Figure 8a). Two isosbestic points are observed at 320 and 375 nm, a pattern similar to those in the related Fp(dppm)$SiMe_3$ complex (isosbestic points at 340 and 395 nm, Figure 8c). The maximum wavelengths of the low-energy bands in **6a/6b** and **7a/7b** are at ∼500 nm, compared to those of the Fp(P−P)EMe_3 complexes at ∼430 nm, presumably an effect associated with the Fc substituent. The ferrocenyl-type redox process observed for **6a** and **7a** at ∼0.5 V exhibits a typical spectral property for an Fc/Fc^+ process, as may be observed for **6b** in Figure 8b. The typical UV/vis spectral changes of Fc/Fc^+ are shown in Figure 8d.

Attempted Chemical Oxidation of 6a and 7a. To investigate this reactivity, we treated complexes **6a** and **7a** to a chemical oxidation reaction using $AgPF_6$. From the reaction mixture we were able to isolate $FcSiMe_2F$ (or $FcGeMe_2F$) in good yield, thereby confirming the facile oxidative cleavage of the Fe−Si/Fe−Ge bonds. $FcSiMe_2F$ (from **6a**)[32] and $FcGeMe_2F$ (from **7a**) were isolated as hexane-soluble products, while the iron compound [CpFe(Ph_2PCH═$CHPPh_2$)]PF_6 was isolated as an acetone-soluble product from the residue of both reactions (Scheme 1).

NMR spectroscopy and elemental analysis confirmed the formation of these products, and ESI mass spectroscopy of $FcGeMe_2F$ revealed $[M]^+$ at *m*/*z* 306 and $[M^+ - F]$ at *m*/*z* 287. Stable $17e^-$ Cp*Fe(dppe) and its $16e^-$ oxidized complex $[Cp^*Fe(dppe)]^+PF_6^-$ have been reported in the literature, and analysis by X-ray crystallography revealed their structures.[33] This further proves that after oxidation the Fe−E bond was not stable and ruptured to form $[FcEMe_2]^+$ species, which takes a fluoride ion from PF_6^- to form $FcEMe_2F$. We have not further studied this aspect of the chemistry, but it is clear that a series of complex processes take place during the electrochemical voltammetry experiments. The second irreversible oxidation observable at ∼0.4 V (**6a**, **6b**, **7a**, and **7b**) presumably belongs to one such material, but we are unable/unwilling to speculate upon its formulation.

(32) Bourke, S. C.; MacLachlan, M. J.; Lough, A. J.; Manners, I. *Chem. Eur. J.* **2005**, *11*, 1989.
(33) Hamon, P.; Toupet, L.; Hamon, J.-R.; Lapinte, C. *Organometallics* **1996**, *15*, 10.

Table 4. Cyclic Voltammetric Data of 5−8[a] and 5a, 6a/b, 7a/b, and 8a[b]

compd	$E_{p,a}$	$E_{p,c}$	$E_{1/2}$
5	0.70	0.41	0.55
	1.65		
5a	−0.17	−0.25	−0.21
	0.62	0.54	0.58
6	0.69	0.39	0.54
	1.70		
6a	0.06	−0.02	0.02
	0.38		
	0.53	0.41	0.47
6b	0.00	−0.07	−0.04
	0.39		
	0.53	0.45	0.49
7	0.74	0.40	0.57
	1.60		
7a	0.08	0.00	0.04
	0.39		
	0.53	0.44	0.49
	0.63	0.55	0.59
7b	−0.01	−0.08	−0.05
	0.38		
	0.57	0.47	0.52
8	0.72	0.43	0.57
	1.75		
8a	−0.20		
	0.03		
	0.60	0.42	0.51
ferrocene	0.54	0.46	0.50

[a] Oxidation potentials (V vs Ag/AgCl, CH_2Cl_2, 0.1 M TBAB). [b] Oxidation potentials (V vs SCE, CH_2Cl_2, 0.1 M TBAP).

Experimental Section

All experiments were performed under an atmosphere of dry N_2 using Schlenk techniques. THF and hexanes were freshly distilled from sodium benzophenone ketyl immediately prior to use; $CH_2[CpFe(CO)_2Me]_2$ (**1**)[13b] and $SiMe_2[(\eta^5\text{-}C_5H_4)Fe(CO)_2Me]_2$ (**2**) were synthesized by following the procedure reported for $SiMe_2[(\eta^5\text{-}C_5H_4)Fe(CO)_2SiMe_2SiMe_3]_2$.[13] $GeMe_2[(\eta^5\text{-}C_5H_4)Fe(CO)_2Me]_2$ (**3**),[14] $SnMe_2[(\eta^5\text{-}C_5H_4)Fe(CO)_2Me]_2$ (**4**),[14] $(\eta^5\text{-}C_5H_5)Fe(CO)_2SiMe_2Fc$ (**6**),[25] and $(\eta^5\text{-}C_5H_5)Fe(dppm)SiMe_3$ (**9**)[11] were prepared according to literature methods. $FcSn^tBu_2Cl$ was prepared by following the procedure reported for $FcSiMe_2Cl$.[26] 1,2-Bis(diphenylphosphino)ethane, *cis*-1,2-bis(diphenylphosphino)ethylene, 1,2-bis(diphenylphosphino)methane, and bis(dimethylphosphino)ethane were purchased from Strem Chemicals and used as received. Tetra-*n*-butylammonium perchlorate (TBAP) and dichloromethane (CH_2Cl_2, 99.5%) were obtained from Fluka Chemical Company and used as received. Other solvents for cyclic voltammetry included benzonitrile (PhCN, 99.0%), dimethyl sulfoxide (DMSO, 99.9%), *N*,*N*-dimethylformamide (DMF, 99.9%), and pyridine (99.9%); these were purchased from Sigma-Aldrich and used without further purification. Cyclic voltammetry was carried out at room temperature under an atmosphere of dry N_2 using a Pine Instrument Co. AFCBP1 potentiostat. A three-electrode system was used and consisted of a platinum-disk or glassy-carbon-disk working electrode, a platinum-wire counter electrode, and a saturated calomel reference electrode (SCE). The SCE was separated from the bulk of the solution by a fritted-glass bridge of low porosity that contained the solvent/supporting electrolyte mixture. UV−vis spectroelectrochemical experiments were performed with an optically transparent platinum thin-layer electrode of the type described in the literature,[34] and the UV−vis spectra were recorded with a HP 8453 diode array spectrophotometer. Infrared spectra were obtained in THF/hexane solution using an ATI Mattson Infinity series FTIR spectrometer; ^1H, ^{13}C, ^{29}Si, and ^{31}P NMR were recorded in C_6D_6 on a Bruker DPX-300 spectrometer at 300, 75.4, 59.6, and 121.5 MHz, respectively, and the values are reported in ppm. Elemental analysis was performed at Galbraith Laboratories.

(34) Lin, X. Q.; Kadish, K. M. *Anal. Chem.* **1985**, *57*, 1498.

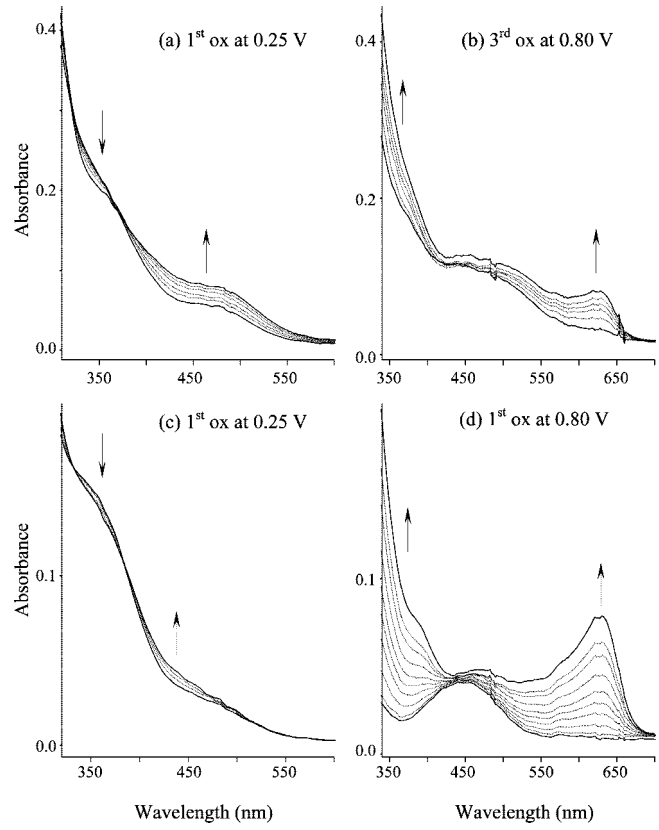

Figure 8. UV/vis spectral changes upon oxidations for $(\eta^5\text{-}C_5H_5)Fe(dppm)SiMe_2Fc$ (a and b), $(\eta^5\text{-}C_5H_5)Fe(dppm)SiMe_3$ (c), and Fc (d) in CH_2Cl_2 and 0.2 M TBAP.

Scheme 1. Oxidative Cleavage of the Fe−Si Bond

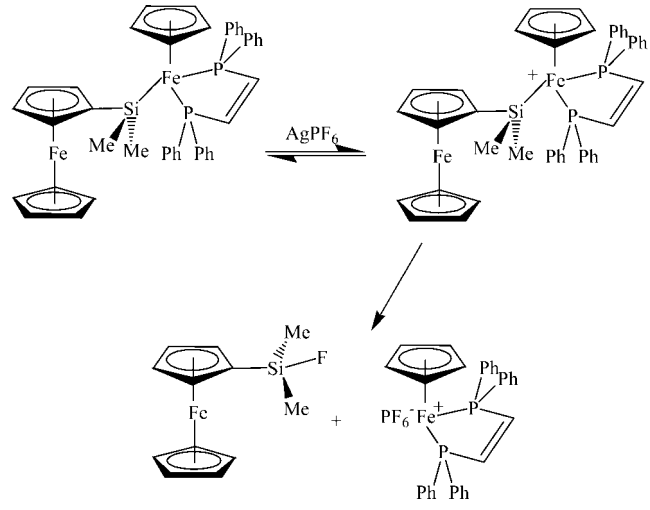

Synthesis of $CH_2[(\eta^5\text{-}C_5H_4)Fe(dppe)Me]_2$ (1a). To a 40 mL THF solution of **1** (0.64 g, 1.62 mmol) in a quartz tube was added 1.28 g (3.24 mmol) of dppe, and the tube was degassed twice. The solution was then irradiated by a Hanovia 450 W medium pressure lamp at a distance of 4 cm for 2−3 days. After completion of the reaction, THF was evaporated under vacuum. The solid material obtained was washed with hexanes and filtered. The hexane-insoluble orange material was collected, dried, and characterized as **1a** (70%). Mp: 138−140 °C. Anal. Calcd for $C_{65}H_{64}P_4Fe_2$: C, 72.23; H, 5.97. Found: C, 72.11; H, 5.90. ^1H NMR: δ −0.50 (6H, FeMe), 1.92 (s, 2H, CH_2), 2.28 (s, 8H, $P(CH_2)_2P$), 3.92 (s, 4H, C_5H_4), 4.37 (s, 4H, C_5H_4), 7.09−7.63 (40H, Ph). ^{13}C NMR: δ −17.0

(t, FeMe, $^2J_{P-C}$ = 26.4 Hz), 22.9 (CH_2), 27.6 (t, $P(CH_2)_2P$, J_{P-C} = 21.5 Hz), 67.7, 75.5, 79.3 (C_5H_4), 129.2, 132.6, 139.1, 144.0 (Ph). ^{31}P NMR: δ 112.3.

2a−**4a** were prepared by a similar procedure and isolated in 65−70% yield. All these compounds were purified by recrystallization from a mixture of benzene and hexanes.

$SiMe_2[(\eta^5\text{-}C_5H_4)Fe(CO)_2Me]_2$ (2).[13] Orange oil. Anal. Calcd for $C_{18}H_{20}Fe_2O_4Si$: C, 49.12; H, 4.58. Found: C, 49.01; H, 4.50. IR (THF, cm^{-1}): 2010, 1956 (ν_{CO}). ^{1}H NMR: δ 0.38 (s, 6H, FeMe), 0.40 (s, 6H, $SiMe_2$), 4.34 (s, 4H, C_5H_4), 4.41 (s, 4H, C_5H_4). ^{13}C NMR: δ −22.5 (FeMe), −0.29 ($SiMe_2$), 84.1, 86.9, 92.1 (C_5H_4). ^{29}Si NMR: δ −10.6.

$SiMe_2[(\eta^5\text{-}C_5H_4)Fe(dppe)Me]_2$ (2a). Mp: 148 °C dec. Anal. Calcd for $C_{66}H_{68}Fe_2P_4Si$: C, 70.47; H, 6.09. Found: C, 69.95; H, 6.10. ^{1}H NMR: δ −0.4 (6H, FeMe), 0.22 (s, 6H, $SiMe_2$), 2.08 (s, 8H, $P(CH_2)_2P$), 4.05 (s, 4H, C_5H_4), 4.75 (s, 4H, C_5H_4), 7.10−7.68 (40H, Ph). ^{13}C NMR: δ −20.3 (t, FeMe, $^2J_{P-C}$ = 26.8 Hz), −0.61 ($SiMe_2$), 27.6 (t, $P(CH_2)_2P$, J_{P-C} = 21.0 Hz), 78.4, 84.3, 87.1 (C_5H_4), 129.3, 131.1, 133.3, 142.0 (Ph). ^{29}Si NMR: δ −5.9; ^{31}P NMR: δ 110.3.

$GeMe_2[(\eta^5\text{-}C_5H_4)Fe(dppe)Me]_2$ (3a). Mp: 150 °C dec. Anal. Calcd for $C_{66}H_{68}Fe_2GeP_4$: C, 67.79; H, 5.86. Found: C, 67.71; H, 5.68. ^{1}H NMR: δ −0.5 (6 H, FeMe), 0.43 (s, 6H, $GeMe_2$), 2.12 (s, 8H, $P(CH_2)_2P$), 4.05 (s, 4H, C_5H_4), 4.74 (s, 4H, C_5H_4), 7.12−7.70 (40H, Ph). ^{13}C NMR: δ −20.2 (t, FeMe, $^2J_{P-C}$ = 27.1 Hz), −1.30 ($GeMe_2$), 27.5 (t, $P(CH_2)_2P$, J_{P-C} = 20.3 Hz), 77.9, 84.5, 89.5 (C_5H_4), 128.7, 132.2, 138.6, 144.4 (Ph). ^{31}P NMR: δ 109.0.

$SnMe_2[(\eta^5\text{-}C_5H_4)Fe(dppe)Me]_2$ (4a). Mp: 162 °C dec. Anal. Calcd for $C_{66}H_{68}Fe_2P_4Sn$: C, 65.21; H, 5.64. Found: C, 65.01; H, 5.51. ^{1}H NMR: δ −0.4 (6H, FeMe), 0.22 (s, 6H, $SnMe_2$), 2.08 (s, 8H, $(CH_2)_2$), 4.05 (s, 4H, C_5H_4), 4.75 (s, 4H, C_5H_4), 7.10−7.68 (40 H, Ph). ^{13}C NMR: δ −19.2 (t, FeMe, $^2J_{P-C}$ = 27.1 Hz), −8.10 ($SnMe_2$), 27.5 (t, $(CH_2)_2$, J_{P-C} = 20.3 Hz), 78.3, 86.5, 87.1 (C_5H_4), 132.2, 132.9, 138.6, 144.5.0 (Ph). ^{119}Sn NMR: δ −27.5. ^{31}P NMR: δ 113.0.

General Synthetic Procedure for Diphosphine Derivatives 5a, 6a/6b, 7a/7b, and 8a. To a 30 mL THF solution of **5** (0.25 g, 0.69 mmol) in a quartz tube was added 0.28 g (0.69 mmol) of cis-dppen, and the tube was degassed twice. The solution was then irradiated by a Hanovia 450 W medium-pressure lamp at a distance of 4 cm for 40−45 h. After completion of the reaction, THF was evaporated under vacuum. The solid material obtained was washed with hexanes and filtered. The hexane-insoluble red material was collected, dried, and characterized as **5a**. Recrystallization from benzene and hexanes (1:2) afforded the pure compound in 68% yield. **6a/6b**, **7a/7b**, and **8a** were prepared by following the identical procedure as described above for **5a** in 65−70% yields.

$(\eta^5\text{-}C_5H_5)Fe(cis\text{-}dppen)Fc$ (5a). Mp: 175−178 °C dec. Anal. Calcd for $C_{41}H_{36}Fe_2P_2$: C, 70.11; H, 5.17. Found: C, 70.01; H, 5.08. ^{1}H NMR: δ 3.77 (s, 2H, Fc), 3.67 (s, 2H, Fc), 4.21 (5H, Fc), 4.54 (5H, C_5H_5), 7.00 (2H, C*H*═C*H*), 7.10−7.62 (20H, Ph). ^{13}C NMR: δ 68.3, 70.0, 73.1 (Fc), 80.7 (C_5H_5), 129.1, 132.6, 133.0, 133.3 (Ph), 148.0 (*C*H═*C*H). ^{31}P NMR: δ 109.0.

$(\eta^5\text{-}C_5H_5)Fe(cis\text{-}dppen)SiMe_2Fc$ (6a). Mp: 192−195 °C dec. Anal. Calcd for $C_{43}H_{42}Fe_2P_2Si$: C, 67.91; H, 5.57. Found: C, 67.80; H, 5.43. ^{1}H NMR: δ 0.16 (s, 6H, $SiMe_2$), 3.40, 4.05, 4.08, 4.29 (14H, C_5H_5 + Fc), 6.92 (2H, C*H*═C*H*), 7.11−7.53 (20H, Ph). ^{13}C NMR: δ 7.88 ($SiMe_2$), 68.5, 68.7, 73.4 (Fc), 78.7 (C_5H_5), 128.7, 129.2, 132.1, 143.1 (Ph), 148.0 (t, *C*H═*C*H, $^1J_{P-C}$ = 33.7 Hz). ^{29}Si NMR: δ 26.0 (t, $^2J_{Si-P}$ = 45.7 Hz). ^{31}P NMR: δ 100.4.

$(\eta^5\text{-}C_5H_5)Fe(dppm)SiMe_2Fc$ (6b). Mp: 180 °C dec. Anal. Calcd for $C_{42}H_{42}Fe_2P_2Si$: C, 67.39; H, 5.66; Found: C, 67.01; H, 5.51. ^{1}H NMR: δ 0.73 (s, 6H, $SiMe_2$), 3.20 (2H, PC*H*$_2$P), 3.95, 4.08, 4.26 (14H, C_5H_5 + Fc), 6.91−7.94 (20H, Ph). ^{13}C NMR: δ 8.69 ($GeMe_2$), 43.4 (t, P*C*H$_2$P, $^1J_{P-C}$ = 20.1 Hz), 68.4, 68.6, 73.8 (Fc), 76.4 (C_5H_5), 129.1, 131.3, 133.5, 143.0 (Ph). ^{29}Si NMR: δ 26.7 (t, $^2J_{Si-P}$ = 44.5 Hz). ^{31}P NMR: δ 39.0.

Synthesis of $(\eta^5\text{-}C_5H_5)Fe(CO)_2GeMe_2Fc$ (7). To a 50 mL THF solution of $[(\eta^5\text{-}C_5H_5)Fe(CO)_2]^-Na^+$ (prepared from 2.0 g (0.011 mol) of $[(\eta^5\text{-}C_5H_5)Fe(CO)_2]_2$) was added, via syringe, 3.6 g (0.011 mol) of $FcGeMe_2Cl$ at 0 °C. The solution was stirred at this temperature for 1 h and then warmed to room temperature and further stirred overnight. The solvent was removed under vacuum, and the residue was extracted with 50 mL of hexanes. The solution was filtered and dried. The residue that was obtained was placed upon a silica column, and elution with hexanes developed a yellow band that was collected, dried, and characterized as **7**. Recrystallization from hexanes afforded pure material in 75% yield. Mp: 114 °C. Anal. Calcd for $C_{19}H_{20}Fe_2GeO_2$: C, 49.11; H, 4.34. Found: C, 49.02; H, 4.35. IR (THF, cm^{-1}): 1987, 1934 (ν_{CO}). ^{1}H NMR: δ 0.92 (s, 6H, $GeMe_2$), 4.05 4.31(m, 14H, C_5H_5 + Fc). ^{13}C NMR: δ 5.21 ($GeMe_2$), 68.5, 70.0, 71.5 (Fc), 83.2 (C_5H_5), 216.2 (CO).

$(\eta^5\text{-}C_5H_5)Fe(cis\text{-}dppen)GeMe_2Fc$ (7a). Mp: 203 °C dec. Anal. Calcd for $C_{43}H_{42}Fe_2GeP_2$: C, 64.15; H, 5.26. Found: C, 64.02; H, 5.30. ^{1}H NMR: δ 0.19 (s, 6H, $GeMe_2$), 4.01−4.39 (m, 14H, C_5H_5 + Fc), 6.90 (2H, C*H*═C*H*), 6.98−7.58 (20H, Ph). ^{13}C NMR: δ 5.85 ($GeMe_2$), 68.0, 68.2, 72.3, (Fc), 77.2 (C_5H_5), 129.2, 131.7, 133.0, 138.1 (Ph), 147.9 (t, *C*H═*C*H, J_{P-C} = 33.7 Hz). ^{31}P NMR: δ 100.9.

$(\eta^5\text{-}C_5H_5)Fe(dppm)GeMe_2Fc$ (7b). Mp: 194 °C dec. Anal. Calcd for $C_{42}H_{42}Fe_2GeP_2$: C, 63.61; H, 5.34. Found: C, 63.52; H, 5.41. ^{1}H NMR: δ 0.76 (s, 6H, $GeMe_2$), 3.23 (2H, PC*H*$_2$P), 4.15−4.51(m, 14H, C_5H_5 + Fc), 6.90−7.41(20H, Ph). ^{13}C NMR: δ 7.54 ($GeMe_2$), 43.3 (t, P*C*H$_2$P, J_{P-C} = 20.3 Hz), 68.2, 68.5, 73.2, (Fc), 75.4 (C_5H_5), 129.2, 131.3, 133.2, 138.9 (Ph). ^{31}P NMR: δ 39.3.

$FcSn^tBu_2Cl$. Anal. Calcd for $C_{18}H_{27}ClFeSn$: C, 47.68; H, 6.00. Found: C, 57.10; H, 5.92. ^{1}H NMR: δ 143 (s, 18H, ^{t}Bu), 4.02, 4.11, 4.30 (9H, Fc). ^{13}C NMR: δ 30.2 (^{t}Bu), 31.9 (*ipso*-^{t}Bu), 68.7, 69.2, 71.4, 74.8, (Fc). ^{119}Sn NMR: δ 72.3.

$(\eta^5\text{-}C_5H_5)Fe(CO)_2Sn^tBu_2Fc$ (8). 8 was synthesized by a procedure similar to that described for **7**. Mp: 122−123 °C. Anal. Calcd for $C_{25}H_{32}Fe_2O_2Sn$: C, 50.47; H, 5.42. Found: C, 50.13; H, 5.19. IR (THF, ν_{CO}, cm^{-1}): 1990, 1935. ^{1}H NMR: δ 1.55 (s, 18H, ^{t}Bu), 4.10, 4.28, 4.37 (14H, C_5H_5 + Fc). ^{13}C NMR: δ 32.7 (^{t}Bu), 33.3 (*ipso*-^{t}Bu), 68.7, 70.1, 74.9, 75.2 (Fc), 81.3 (C_5H_5), 216 (CO). ^{119}Sn NMR, 167.0.

$(\eta^5\text{-}C_5H_5)Fe(dmpe)Sn^tBu_2Fc$ (8a). Mp: 166 °C dec. Anal. Calcd for $C_{29}H_{48}Fe_2P_2Sn$: C, 50.55; H, 7.02. Found: C, 50.20; H, 6.87. ^{1}H NMR: δ 0.95 (6H, PMe_2), 1.46 (4H, $P(CH_2)P$), 1.75 (s, 18H, ^{t}Bu), 4.09, 4.19, 4.34 (14H, C_5H_5 + Fc). ^{13}C NMR: δ 24.5 (P*C*H$_3$), 26.0 (t, P(*C*H$_2$)$_2$P, J_{P-C} = 12 Hz), 30.2 (*ipso*-^{t}Bu), 35.1 (^{t}Bu), 69.0, 69.1, 72.9 (Fc), 76.0 (C_5H_5). ^{119}Sn NMR: δ 105.2 (t, $^2J_{Sn-P}$ = 409 Hz). ^{31}P NMR, 69.3.

Reaction of 6a/7a with $AgPF_6$. To a 30 mL dichloromethane solution of **6a** (0.1 g, 0.13 mmol) was added $AgPF_6$ (0.033 g, 0.13 mmol or 0.065 g, 0.26 mmol) at 0 °C. The formation of black precipitate was observed during the addition of the $AgPF_6$ in each case. The contents were then stirred for 1 h, and dichloromethane was evaporated under vacuum. Extraction of the residue with hexane yielded the previously reported $(\eta^5\text{-}C_5H_5)Fe(\eta^5\text{-}C_5H_4SiMe_2F)$[31] as a yellow solid product purified via a small silica column and characterized by NMR spectroscopy. The remaining residue was dissolved in acetone and filtered; removal of the acetone from the filtrate yielded $[(\eta^5\text{-}C_5H_5)Fe(Ph_2PCH{=}CHPPh_2)]^+PF_6^-$ as a dark red solid. This compound was purified by washing with benzene until the unreacted **6a** was washed away. The reaction of **7a** with $AgPF_6$ was performed in a similar way and yielded $(\eta^5\text{-}C_5H_5)Fe(\eta^5\text{-}C_5H_4GeMe_2F)$ and $[CpFe(Ph_2PCH{=}CHPPh_2)]^+PF_6$.

$(\eta^5\text{-}C_5H_5)Fe(\eta^5\text{-}C_5H_4GeMe_2F)$. Mp: 66−67 °C. Anal. Calcd for $C_{12}H_{15}FFeGe$: C, 46.99; H, 4.93. Found: C, 46.95; H, 4.85. ^{1}H NMR (C_6D_6): δ 0.62 (d, 6H, $GeMe_2$, $^3J_{H-F}$ = 6.0 Hz), 4.03 (5H, Cp, Fc), 4.15 (2H, C_5H_4), 4.22 (2H, C_5H_4). ^{13}C NMR (C_6D_6): δ 0.39

(d, $GeMe_2$, $^2J_{C-F} = 16.0$ Hz), 68.6 (C_5H_5), 71.5 (C_5H_4), 72.6 (C_5H_4). ESI (MS): *m/z* 306.0 (M^+), 287.0 ($M^+ - F$).

(η^5-C_5H_5)Fe($Ph_2PCH{=}CHPPh_2$)]$^+PF_6^-$. Mp: 178−182 °C dec. Anal. Calcd for $C_{31}H_{27}F_6FeP_3$: C, 56.22; H, 4.11. Found: C, 55.45; H, 4.01. ^{1}H NMR (acetone-d_6): δ 4.93 (s, 5H, C_5H_5), 7.18 (2H, CH═CH), 7.26−7.80 (20H, Ph). ^{13}C NMR (acetone-d_6): 90.6 (C_5H_5), 134.6, 136.5, 137.7, 138.6 (Ph), 150.8 (CH═CH). ^{31}P NMR (acetone-d_6): −137.0 (septet, PF_6^-, $^1J_{P-F} = 710.0$ Hz), 105.0 (PCH═CHP).

X-ray Crystallography

Crystals of **6b** and **9** suitable for X-ray analysis were mounted in a Bruker APEX CCD diffractometer equipped with monochromated Mo Kα radiation. Crystallographic measurements were carried out at 296(2) K. Details of the crystal data and refinement parameters are described in Table 1. The structure was solved by direct methods and refined by full-matrix least squares on F^2 values for all reflections using the SHELXL-97 program. All non-hydrogen atoms were assigned anisotropic displacement parameters, and hydrogen atoms were constrained to ideal geometries with fixed isotropic displacement parameters.

Acknowledgment. Financial support from the Welch Foundation (Grant Nos. AH-546 and A0-0001) and an NIH SCORE grant are gratefully acknowledged.

Supporting Information Available: CIF files giving crystallographic data for **6b** and **9** and figures detailing the UV/vis spectroelectrochemistry of **1a** and **4a** and a correlation between the dielectric constant. This material is available free of charge via the Internet at http://pubs.acs.org. Crystal data are also available from the Cambridge Crystallographic Database as file numbers CCDC 661327 (for **6b**) and 661328 (for **9**).

OM8004004